

CERN-TH/2003-213

CPT-2003/PE 4569

DESY 03-135

MPP-2003-74

Lattice QCD in the $\bar{\Lambda}$ -regime and random matrix theory

L. Giusti^{2,1}, M. Luscher¹, P. Weisz², H. Wittig³¹CERN, Theory Division, CH-1211 Geneva 23, Switzerland²Max-Planck-Institut für Physik, Fohringer Ring 6, D-80805 Munich, Germany³DESY, Theory Group, Notkestrasse 85, D-22603 Hamburg, Germany

Abstract

In the $\bar{\Lambda}$ -regime of QCD the main features of the spectrum of the low-lying eigenvalues of the (euclidean) Dirac operator are expected to be described by a certain universality class of random matrix models. In particular, the latter predict the joint statistical distribution of the individual eigenvalues in any topological sector of the theory. We compare some of these predictions with high-precision numerical data obtained from lattice QCD for a range of lattice spacings and volumes. While no complete matching is observed, the results agree with theoretical expectations at volumes larger than about 5 fm^4 .

1. Introduction

The proposition that the low-lying eigenvalues of the Dirac operator in the so-called $\bar{\Lambda}$ -regime of QCD [1,2] are distributed in the same way as the eigenvalues of a large random matrix was put forward a number of years ago [3{5] and has since then been worked out in great detail (see refs. [6,7] for a review and further references). Perhaps the most important qualitative prediction of random matrix theory is that, at vanishing quark masses, the eigenvalues scale proportionally to $(V)^{-1}$, where $\langle \bar{\psi}\psi \rangle$ denotes the (bare) quark condensate and V the space-time volume. In particular, the spectrum near the origin rapidly becomes very dense when the volume increases.

² On leave from CNRS, Centre de Physique Théorique, F-13288 Marseille, France

So far the correctness of the proposition has not been established from first principles. Apart from symmetry and universality arguments, it is supported by chiral perturbation theory, where the Leutwyler-Smilga sum rules [2] can be shown to be reproduced, at large volumes, by random matrix theory. To date there is, however, no similar theoretical check on the distributions of the individual eigenvalues [8,9].

Random matrix theory is well defined for any number $N_{\text{sea}} \geq 0$ of sea quarks. It is thus possible to extend the proposition to quenched QCD, even though the latter tends to be singular in the chiral limit. Another instance where random matrix theory with $N_{\text{sea}} = 0$ may be expected to apply is full QCD with quark masses m such that $m \gg 1$. The quark determinant is safely bounded from below in this case, and the distributions of the low-lying eigenvalues of the massless Dirac operator should consequently be as in quenched QCD (up to a scale transformation).

The present paper is part of an ongoing project whose final goal is to extract physical parameters, such as the pion decay constant and the electroweak effective couplings, from numerical simulations of lattice QCD in the ϵ -regime [10,11]. Since chiral symmetry plays a central rôle in this context, we use a lattice Dirac operator that satisfies the Ginsparg-Wilson relation and thus preserves the symmetry [12–20]. Unfortunately numerical simulations of full QCD then become even more demanding than they normally are, and in this paper we shall, therefore, only consider the case of quenched QCD.

Comparisons of random matrix theory with simulation data obtained from lattice QCD with exact chiral symmetry have previously been published by a number of collaborations [21–24]. Here we extend these studies to significantly larger lattices and collect data at different lattice spacings so as to be able to check for lattice effects. We wish to add that simulations in the ϵ -regime of QCD become increasingly difficult at large volumes, because the low-lying eigenvalues of the Dirac operator are extremely small and closely spaced. The use of efficient techniques such as those described in ref. [10] is thus essential.

2. Random matrix model

To set up notations, we now briefly recall the definition of the matrix model that is expected to describe the spectrum of the Dirac operator in QCD. There is actually a whole universality class of such models, and we will only describe the simplest representative, the so-called gaussian chiral unitary model.

Let us consider $N \times N$ matrices of the form

$$\hat{D} = \begin{pmatrix} 0 & W & gN_+ \\ W^\dagger & 0 & gN_- \end{pmatrix}; \quad N = N_+ + N_-; \quad (2.1)$$

where W is a complex rectangular random matrix. We use the symbol \hat{D} to indicate that the matrix represents the massless Dirac operator in the matrix model. It is then natural to think of N as the space-time volume (times some proportionality constant), while the block structure of \hat{D} is interpreted as a chiral decomposition. Moreover, since any matrix of this form has N_+ chiral zero modes, the index

$$= N_+ - N_- \quad (2.2)$$

may be identified with the topological charge in QCD.

The observables O in the matrix model are arbitrary functions of matrix elements of W , and we are interested in the large- N limit of the expectation values

$$\langle O \rangle = \frac{1}{Z} \int dW \int d\bar{W} \det(\hat{D} + m)^{N_{\text{sea}}} e^{-\frac{1}{2} N \text{tr} W^\dagger W} g \quad (2.3)$$

at fixed $m = mN$. Clearly m represents the quark mass in the matrix model (in the case where all quarks have the same mass), but this parameter is actually irrelevant in the present paper, since we shall compare the matrix model with quenched QCD and thus set $N_{\text{sea}} = 0$ from the beginning.

Apart from the chiral zero modes, all eigenvalues of \hat{D} come in complex conjugate pairs $\pm i_k$ that can be ordered according to

$$0 < i_1 < i_2 < \dots \quad (2.4)$$

The expectation values of these eigenvalues scale proportionally to $1/N$. In particular, the spectral densities at fixed topology,

$$\rho_k(z) = \lim_{N \rightarrow \infty} \langle \text{tr} (\hat{D} - i_k N)^{-1} \rangle; \quad 0 < z < 1; \quad (2.5)$$

as well as the corresponding joint distributions of the first n eigenvalues are well defined and analytically calculable [8,9]. Using these expressions, the expectation values of the first few eigenvalues and of their products can be obtained exactly, although in practice the formulae rapidly become so complicated that numerical methods are required.

3. Numerical simulation

We assume that the reader is familiar with the standard formulations of lattice QCD and the Ginsparg-Wilson relation as discussed in refs. [16-20], for example. In this section we summarize the parameter choices that we have made and discuss what precisely is being compared with random matrix theory.

3.1 Lattice theory

We consider four-dimensional lattices of size L in all dimensions and impose periodic boundary conditions on the fields. The action of the $SU(3)$ gauge field is taken to be the standard plaquette action with bare coupling g_0 . As already mentioned, the lattice Dirac operator D should satisfy the Ginsparg-Wilson relation,

$$\gamma_5 D + D \gamma_5 = a D \gamma_5 D ; \quad (3.1)$$

in addition to the usual requirements such as locality. For this study we decided to use the Neuberger Dirac operator [18], with shift parameter $s = 0.4$ [20], in view of its relative simplicity. The parameter a in eq. (3.1) is then given by

$$a = a/(1 + s); \quad (3.2)$$

where a denotes the lattice spacing (our notational conventions are as in refs. [10,20]).

As usual we define the index of D to be the difference $n_+ - n_-$ of the numbers of exact zero modes with positive and negative chirality. A well-known implication of the Ginsparg-Wilson relation is that $\text{Index} D = Q$, where

$$Q = a^4 \sum_x q(x); \quad q(x) = \frac{1}{2} a \text{tr} \gamma_5 D(x;x) g; \quad (3.3)$$

can be taken as the definition of the topological charge of the gauge field [17]. In particular, the charge density $q(x)$ is a local gauge-invariant expression in the link variables [20].

3.2 Numerical techniques

At large volumes the low-lying non-zero eigenvalues of D are orders of magnitude smaller than the largest eigenvalues. It is hence important to choose a numerical implementation of the Neuberger Dirac operator, where the approximation errors can be guaranteed to be sufficiently small for the spectrum to be obtained to the required level of precision.

Table 1. Simulation parameters

lattice		L=a	r ₀ =a	L [fm]	N _{meas}
A ₁	6:0	12	5:368	1:12	2452
A ₂	6:1791	16	7:158	1:12	1138
B ₀	5:8458	12	4:026	1:49	2918
B ₁	6:0	16	5:368	1:49	1001
B ₂	6:1366	20	6:710	1:49	963
C ₀	5:8784	16	4:294	1:86	1109
C ₁	6:0	20	5:368	1:86	931

The minimal polynomial approximation that was introduced in ref. [10] provides a solution to this problem. We also apply some of the other numerical techniques mentioned there. In particular, the eigenvalues of D are obtained by minimization of the Ritz functional [25,26] of the hermitian operators

$$D_{\pm} = P D P^{\dagger}; \quad P = \frac{1}{2} (1 \pm \gamma_5); \quad (3.4)$$

in the positive and negative chirality sectors.

3.3 Simulation parameters

We have simulated altogether 7 lattices with various sizes and lattice spacings (see table 1). There are three groups of lattices, labelled A, B and C, where the lattice size L is kept fixed in physical units. Within each of these groups, the bare coupling $\beta = 6/g_0^2$ is thus the only parameter that varies, which allows us to obtain a direct check on the dependence of the calculated observables on the lattice spacing. For the conversion to physical units we use the recent parametrization of the Sommer scale r_0 [27] by the ALPHA collaboration (eq. (2.6) of [28]) and set $r_0 = 0.5 \text{ fm}$.

In all these simulations the generation of the gauge-field configurations consumes a negligible amount of computer time. We have therefore performed many update cycles between subsequent configurations (typically 500 iterations of 1 heatbath and at least 6 over-relaxation updates of all link variables) so that they can be assumed to be statistically independent. The number of gauge fields in each ensemble quoted in the last column of table 1 coincides with the number of "measurements" of the topological charge and the lowest few eigenvalues of the Dirac operator.

3.4 Matching with random matrix theory

The eigenvalues of D lie on a circle in the complex plane,

$$D = \frac{1}{a} \sum_{j=1}^N e^{i\theta_j}; \quad \theta_j = \frac{1}{a} \left(1 - \cos \theta_j \right); \quad (3.5)$$

and come in complex conjugate pairs (if Im does not vanish). We cannot directly compare these eigenvalues with the eigenvalues of the random matrix \hat{D} since the latter lie on the imaginary axis. The important point to note is, however, that the radius of the circle diverges in the continuum limit and that the real parts of the eigenvalues with $j \ll N$ rapidly go to zero in this limit. In practice we set (for these eigenvalues)

$$\theta_j = \frac{1}{a} \sqrt{2 \left(1 - \cos \theta_j \right)} \quad (3.6)$$

and compare the distributions of the scaled eigenvalues

$$z = \frac{1}{a} \theta_j; \quad V = L^4; \quad (3.7)$$

with those of the scaled eigenvalues $z = \frac{1}{a} \theta_j$ in the matrix model. Evidently the definition (3.6) is arbitrary to some extent, but other suggested formulae differ by terms of order a^2 and are thus asymptotically equivalent. In particular, for the analysis of our data this ambiguity turns out to be numerically insignificant.

Although we use the same symbol for the proportionality constant in eq. (3.7) as for the quark condensate in full QCD, it should be emphasized that in the present context χ is just a free parameter with no obvious physical interpretation. The quark condensate is actually not even well defined in quenched QCD, since it is not possible to pass to the chiral limit in this theory. We thus prefer to regard χ as an effective parameter that is to be determined, on any given lattice, by comparing the spectral distributions of D with those of \hat{D} .

4. Distribution of the topological charge

We now first discuss the probability P to find a gauge field with topological charge $Q = \frac{1}{2} \int \text{Tr} F \wedge F$. Random matrix theory does not provide any information on P , and we are thus uniquely concerned with properties of QCD in this section. Basically we

wish to find out whether the charge distribution scales in the expected way as a function of the volume and the lattice spacing. If this is the case, it will then be more plausible that the eigenvalues of the Dirac operator behave coherently in the different sectors (as suggested by random matrix theory).

4.1 Large volume limit

The fact that the topological charge Q is given in terms of a local density $q(x)$ allows us to derive an asymptotic formula for P at large volumes. First note that since Q is integer-valued, we have

$$P = \frac{1}{2} \int_{-\infty}^{\infty} d\theta e^{i\theta Q} e^{-F(\theta)}; \quad F(\theta) = -\ln \int e^{i\theta Q} \quad (4.1)$$

Using the moment-cumulant transformation, the free energy $F(\theta)$ may then be expanded in a series

$$F(\theta) = V \sum_{n=1}^{\infty} \frac{\theta^{2n}}{(2n)!} C_n; \quad (4.2)$$

$$C_n = a^{8n-4} \int \prod_{i=1}^{2n} dx_i h_q(x_i) \dots q(x_{2n-1}) q(0) i^{\text{con}}; \quad (4.3)$$

In quenched QCD the connected correlation functions in this formula are evaluated in the pure gauge theory, where all particles are fairly heavy (the mass of the lightest glueball is around 1.6 GeV). As a result the cumulants C_n approach their infinite-volume limit exponentially fast, i.e. as soon as L is larger than 1 fm or so, they can be expected to be practically independent of the volume.

If we now insert eq. (4.2) in eq. (4.1), it is clear that the integral is dominated by the saddle point at $\theta = 0$ in the large-volume limit. The asymptotic formula

$$P = \frac{e^{-\frac{Q^2}{2}}}{2} (1 + O(V^{-1})) \quad (4.4)$$

is thus obtained, where $Q^2 = \langle Q^2 \rangle$. On the lattices $A_1 \dots C_1$, the observed charge distributions are in fact statistically consistent with the leading term in eq. (4.4) (see g.1). From this point of view the lattices are hence in the large-volume regime.

Y As in the matrix model, expectation values in QCD at fixed charge $Q =$ are denoted by $\langle \dots \rangle_Q$. Brackets without lower index imply an unconstrained expectation value and $\langle \dots \rangle_Q^{\text{con}}$ stands for the connected part of the full n -point correlation function of the fields $\psi_1 \dots \psi_n$.

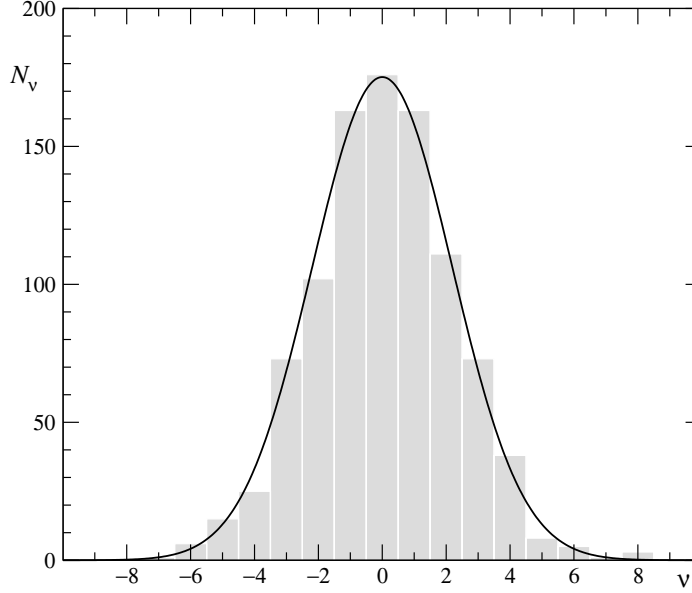


Fig. 1. Histogram of the topological charge on lattice B_2 . The curve represents the leading term in the large-volume formula (4.4) with $\chi^2 = hQ^2i$ taken from table 2.

4.2 Determination of the topological susceptibility

The width of the charge distribution (or, equivalently, the susceptibility $\chi^2 = hQ^2i/V$) may be calculated straightforwardly by averaging Q^2 over the ensemble of gauge configurations that was generated. However, this procedure may not be safe in general, because the tails of the charge distribution are poorly sampled.

To understand what the problem is, first note that the number N of configurations with charge $Q = \nu$ in a sample of N configurations is distributed according to Poisson statistics. In particular, the variance of N is equal to its mean value $N P_\nu$. If N is small, the empirical probability N/N may consequently be quite different from the true probability P_ν . We thus compute hQ^2i as a sum of two contributions,

$$\sum_{j=-j_{\max}}^{j_{\max}} \nu^2 \frac{N_\nu}{N} + \sum_{j=j_{\max}}^{j_{\max}} \nu^2 P_\nu; \quad (4.5)$$

where j_{\max} is the maximal charge such that $N_\nu + N_{-\nu}$ is at least 10 for all ν in the first sum. To evaluate the second sum, we insert the large-volume expression (4.4) for the exact distribution P_ν , setting χ^2 to the naive estimate of hQ^2i , where any exceptional configurations with absolute charges $|Q|$ significantly larger than j_{\max}

Table 2. Topological susceptibility

	A ₁	A ₂	B ₀	B ₁	B ₂	C ₀	C ₁
$\langle Q^2 \rangle$	1:63 (5)	1:59 (8)	5:6 (2)	5:6 (3)	4:8 (2)	15:0 (7)	12:8 (9)
r_0^4	0:065 (2)	0:064 (3)	0:071 (2)	0:071 (4)	0:061 (3)	0:078 (4)	0:066 (5)

The errors quoted in the second row do not include the error on $r_0=a$

should be discarded (there were none in our samples). The second sum is actually a small correction to the first, and other estimates of $\langle Q^2 \rangle$ could therefore be used at this point with little effect on the results listed in table 2.

The fact that r_0^4 comes out to be the same within errors on the lattices A₁;B₁ and C₁ (which have exactly the same lattice spacing but different volumes) is in line with the above argumentation that finite-volume effects in connected correlation functions of local fields should be small in the pure gauge theory when $L \gg 1 \text{ fm}$. As far as the volume dependence is concerned, the charge distribution on the lattices that we have simulated thus behaves entirely according to expectations.

4.3 Continuum limit

It is often taken for granted that the division of the space of gauge fields into topological sectors and the topological susceptibility have a well-defined meaning in the continuum limit of QCD. Beyond the semi-classical approximation, where the functional integral is expanded about the instanton solutions, the question remains undecided, however, and is in fact difficult to pose in precise terms without reference to a regularization of the theory. In particular, the susceptibility cannot simply be defined as the integral over the two-point function $\langle q(x)q(0) \rangle$ of the charge density, because there is a non-integrable singularity at $x = 0$.

In lattice QCD the space of fields is connected and the assignment of a topological charge to every lattice gauge field is consequently not unique. The definition (3.3), for example, depends on the choice of D . Close to the continuum limit, the integration measure in the functional integral may, however, be increasingly supported on fields where the charge assignment is unambiguous. The topological sectors would

^y To the extent they can be compared, the results obtained in a similar study of the topological susceptibility by DelDebbio and Pica [29], which appeared during the completion of the present paper, are compatible with those reported here.

then arise dynamically and any differences in the definition of the charge would be ultimately irrelevant.

This picture suggests that the susceptibility should behave like a physical quantity of dimension 4, i.e. that the combination r_0^4 should be independent of the lattice spacing, up to corrections of order a^2 . The data listed in the second row of table 2 may actually be fitted by the linear expression $r_0^4 = c_0 + c_1 a^2$, and our results are, therefore, statistically consistent with the existence of a well-defined continuum limit of the topological susceptibility. If we fit the data from the B lattices only, taking the error on $r_0=a$ into account [28], the value $r_0^4 = 0.059(5)$ is obtained at $a = 0$, but this number should evidently be used with caution, as it is determined by linear extrapolation in a^2 of only three data points.

5. Comparison with random matrix theory

As discussed in subsect. 3.4, the matching of the QCD spectra with random matrix theory involves an unknown scale that must be determined from the data. This complication can be avoided by considering ratios of expectation values, and we now look at some of these first.

5.1 Scale-independent tests

In table 3 we list our results for the ratios $h_{ki} = h_{ji}$ on the lattices $A_1; \dots; C_1$. There is a significant cancellation of statistical errors when the ratios are formed, particularly for the larger values of k and j . For this reason we show the data for all $1 \leq j < k \leq 4$, even though some of them are related to each other. The figures in the last column of table 3 are the values of the ratios predicted by random matrix theory [8,9].

A number of observations can be made at this point:

- (1) For fixed physical volume (i.e. within the groups of lattices A, B or C), the data on each line are constant within 1 or, in rare cases, at most 2 standard deviations. In other words, there is no statistically significant dependence on the lattice spacing in these ratios.
- (2) In all topological sectors the results obtained on the lattices B agree with random matrix theory. There are deviations at the level of 2 or 3 standard deviations in a few places, but this has to be so by the laws of statistics.

Table 3. Simulation results for the ratios $h_{ki} = h_{ji}$

	k=j	A ₁	A ₂	B ₀	B ₁	B ₂	C ₀	C ₁	RM T
0	2=1	2.29 (4)	2.28 (6)	2.71 (6)	2.73 (10)	2.56 (10)	2.77 (12)	3.01 (14)	2.70
0	3=1	3.29 (7)	3.25 (9)	4.45 (11)	4.59 (18)	4.43 (18)	4.65 (22)	4.89 (23)	4.46
0	4=1	4.07 (8)	4.00 (11)	6.25 (15)	6.55 (26)	6.15 (26)	6.67 (31)	6.99 (34)	6.22
0	3=2	1.44 (1)	1.42 (2)	1.65 (2)	1.68 (3)	1.73 (3)	1.68 (4)	1.63 (4)	1.65
0	4=2	1.78 (2)	1.75 (2)	2.31 (3)	2.40 (5)	2.40 (5)	2.41 (6)	2.32 (6)	2.30
0	4=3	1.24 (1)	1.23 (1)	1.40 (1)	1.43 (2)	1.39 (2)	1.44 (2)	1.43 (2)	1.40
1	2=1	1.78 (2)	1.73 (3)	2.04 (3)	2.04 (4)	2.12 (4)	2.03 (5)	1.95 (5)	2.02
1	3=1	2.35 (3)	2.27 (4)	3.08 (4)	3.08 (6)	3.23 (7)	3.13 (8)	2.97 (7)	3.03
1	4=1	2.80 (3)	2.69 (4)	4.06 (6)	4.08 (9)	4.30 (9)	4.27 (11)	4.15 (10)	4.04
1	3=2	1.32 (1)	1.31 (1)	1.51 (1)	1.51 (2)	1.53 (2)	1.55 (2)	1.53 (2)	1.50
1	4=2	1.57 (1)	1.56 (1)	1.99 (2)	2.00 (3)	2.03 (3)	2.11 (3)	2.13 (4)	2.00
1	4=3	1.19 (1)	1.19 (1)	1.32 (1)	1.32 (1)	1.33 (1)	1.36 (2)	1.40 (2)	1.33
2	2=1	1.55 (2)	1.55 (3)	1.80 (2)	1.83 (4)	1.80 (4)	1.84 (4)	1.82 (3)	1.76
2	3=1	1.98 (3)	1.95 (4)	2.55 (3)	2.60 (6)	2.51 (6)	2.66 (6)	2.66 (5)	2.50
2	4=1	2.28 (3)	2.27 (5)	3.26 (4)	3.30 (8)	3.23 (8)	3.50 (8)	3.51 (7)	3.24
2	3=2	1.28 (1)	1.26 (1)	1.42 (1)	1.42 (2)	1.39 (2)	1.44 (2)	1.46 (2)	1.42
2	4=2	1.48 (1)	1.47 (2)	1.82 (2)	1.80 (3)	1.79 (3)	1.90 (3)	1.93 (3)	1.83
2	4=3	1.16 (1)	1.16 (1)	1.28 (1)	1.27 (1)	1.29 (1)	1.32 (1)	1.32 (1)	1.29

(3) The results on the lattices C are also matched by random matrix theory, although in this case some differences of up to 4 standard deviations are observed at $\beta = 1$ and $\beta = 2$. It is still possible that these are caused by an unlikely statistical fluctuation, particularly so since they do not appear to follow any obvious systematic trend.

(4) In the case of the lattices A, on the other hand, the data are in clear disagreement with random matrix theory. Since the ratios are practically independent of the lattice spacing, we conclude that we are seeing the onset of finite-volume effects that are specific to QCD and are not accounted for by random matrix theory. Such a regime must in any case eventually be reached when L is set to values below 1 fm.

For illustration the ratios calculated on lattice B₂ are plotted in fig. 2 together

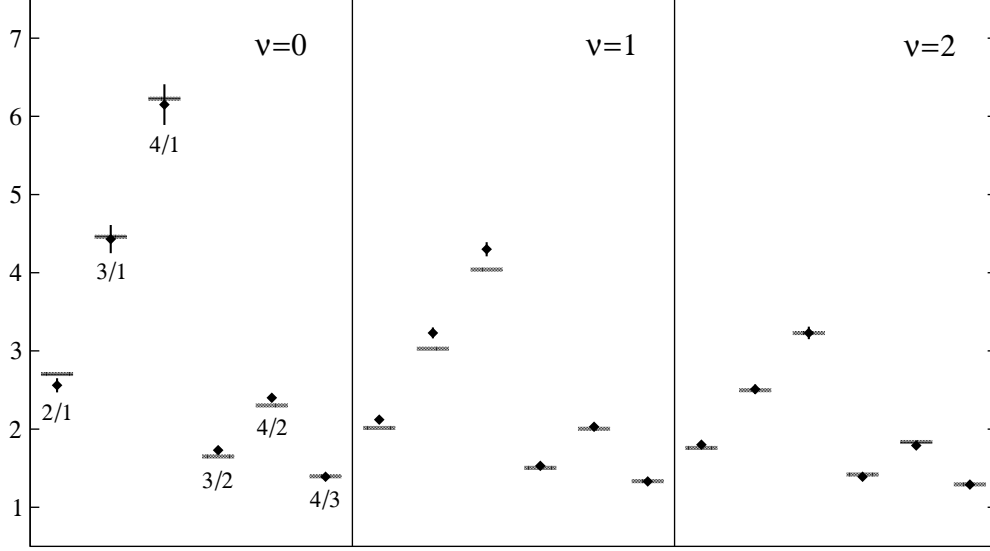


Fig.2. Comparison of simulation results for $h_k i = h_j i$ from lattice B_2 (diamonds) with random matrix theory (horizontal bars) in the sectors with topological charge $= 0;1;2$.

with the values predicted by random matrix theory. This shows rather clearly that the observed matching is non-trivial and at a high level of precision. Evidently expectation values of products of eigenvalues could also be considered, but it is our experience that ratios involving these are obtained with relatively large statistical errors, and comparisons with random matrix theory are consequently less compelling.

5.2 Calculation of

In the present context λ is considered to be a parameter with no independent physical meaning whose value may be fixed by imposing a suitable normalization condition. We may, for example, require the relation

$$h_k i^{QCD} V = h z_k i^{RMT} \quad (5.1)$$

to hold exactly for some k and V , where z_k denotes the k th scaled eigenvalue in the random matrix model (cf. subsect. 3.4). The numbers obtained in this way are listed in table 4.

In the case of the lattices A_1 and A_2 , we already know that the eigenvalue distributions in QCD are poorly matched by those in random matrix theory. The results

Table 4. Values of r_0^3 determined from h_k

	k	A_1	A_2	B_0	B_1	B_2	C_0	C_1
0	1	0.215 (5)	0.242 (8)	0.221 (5)	0.274 (12)	0.280 (13)	0.263 (13)	0.332 (18)
0	2	0.254 (3)	0.287 (4)	0.220 (3)	0.271 (7)	0.297 (8)	0.257 (6)	0.298 (9)
0	3	0.291 (2)	0.332 (3)	0.221 (2)	0.266 (5)	0.283 (5)	0.253 (5)	0.302 (7)
0	4	0.329 (2)	0.377 (2)	0.220 (2)	0.260 (3)	0.284 (4)	0.246 (4)	0.295 (6)
1	1	0.244 (3)	0.263 (5)	0.223 (3)	0.268 (7)	0.306 (7)	0.271 (9)	0.290 (8)
1	2	0.276 (2)	0.307 (3)	0.220 (2)	0.266 (4)	0.292 (4)	0.270 (4)	0.300 (6)
1	3	0.315 (2)	0.352 (2)	0.219 (2)	0.264 (3)	0.287 (3)	0.262 (4)	0.296 (5)
1	4	0.352 (2)	0.395 (2)	0.222 (2)	0.266 (3)	0.288 (3)	0.257 (3)	0.282 (4)
2	1	0.265 (4)	0.298 (7)	0.228 (3)	0.273 (7)	0.291 (8)	0.275 (7)	0.312 (7)
2	2	0.301 (3)	0.340 (4)	0.224 (2)	0.262 (5)	0.284 (5)	0.262 (6)	0.301 (5)
2	3	0.335 (2)	0.382 (3)	0.223 (2)	0.262 (4)	0.289 (4)	0.258 (4)	0.293 (5)
2	4	0.374 (2)	0.425 (3)	0.226 (2)	0.267 (3)	0.291 (3)	0.253 (3)	0.287 (4)

The errors quoted in this table do not include the error on $r_0=a$

for r_0 consequently show a strong dependence on k and a , and any normalization convention that one may adopt is therefore rather arbitrary. The situation looks much better on the lattices $B_0; \dots; C_1$, where the calculated values of r_0^3 are practically the same for all k and a (i.e. in each column of table 4). Up to the quoted errors, r_0^3 is thus consistently determined in these cases.

There is, however, no reason to expect the dimensionless combination r_0^3 to be independent of the lattice spacing and the lattice size. In particular, at fixed lattice spacing, r_0^3 appears to be monotonically increasing with the volume. Close to the continuum limit, r_0^3 presumably renormalizes like the scalar quark density S , so that

$$Z_S r_0^3 = h(g_0; L) + O(a^2); \quad (5.2)$$

where $Z_S(g_0; a)$ denotes a renormalization constant, m the renormalization mass and L the associated renormalization-group invariant scale. The analogy with full QCD suggests this, and, more importantly, the fact that the higher-order cumulants of S (which renormalize multiplicatively) are directly related to the spectral density of the Dirac operator [2].

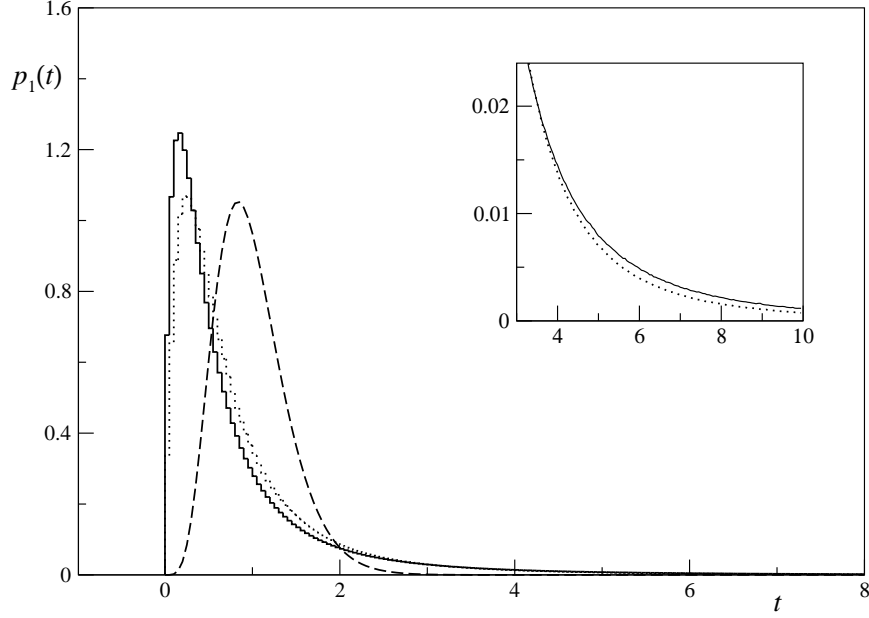


Fig. 3. Probability distribution $p_1(t)$ of the local magnitude $t = \sum_{i=1}^4 (\mathbf{x}_i)^2 V$ of the first normalized eigenvector of $P_+ D^y D P_+$ in the charge $Q = 0$ sector. The solid and dotted lines are the distributions obtained on the lattices C_1 and B_2 respectively, while the dashed curve is what would be expected for a random vector with unit norm.

The renormalization factor Z_S connecting the lattice theory to the \overline{MS} scheme of dimensional regularization has been calculated to one-loop order of perturbation theory [30,31]. This formula is unfortunately not very useful in the present context, because it largely underestimates the true value of the renormalization constant

$$Z_S|_{\mu=2\text{ GeV}} = 1.43(11) \quad \text{at} \quad \beta = 6.0; \quad (5.3)$$

which is obtained from non-perturbative scaling studies [32]. As a consequence, and since Z_S is (for $s = 0:4$) currently only known at this value of β , we are unable to study the scaling behaviour of $Z_S r_0^3$. More extensive simulations would in any case be required for a reliable extrapolation to the continuum limit (if eq. (5.2) holds).

5.3 Local magnitude of the low modes

In correlation functions of local operators such as the pseudo-scalar and the scalar quark densities, the contribution of the low modes of the Dirac operator can be large, owing to the presence of uncanceled factors of $1/\lambda_k$. The actual size of these

contributions also depends on the magnitude $\|j_k(x)\|^2$ of the associated normalized eigenfunctions $j_k(x)$ at the points x where the operators sit.

In fig. 3 we show the distribution of the local magnitude of the lowest mode in the vacuum sector. Although an average over many gauge configurations is plotted, this curve is actually fairly universal, i.e. fluctuations are small and very similar results are obtained for the higher modes and in the other topological sectors. Random matrix theory does not refer to an underlying local structure and is hence not expected to be relevant here. In the two chirality sectors, the eigenvectors of $\hat{D}^{\gamma}\hat{D}^{\delta}$ are in fact uniformly distributed random vectors, and the associated distribution (which is also displayed in the figure) is clearly different from the one in QCD.

An interesting aspect of the QCD distribution shown in fig. 3 is that it decreases only relatively slowly at large local magnitudes t . The inset in the figure shows this in greater detail. In particular, the probability to find a point on the lattice where $t \geq 3$ is more than 5%, and there is still a non-negligible probability of nearly 0.6% for having $t \geq 10$. Correlation functions of local operators in the β -regime may consequently suffer from large statistical fluctuations that derive from the presence of exceptionally low eigenvalues of the Dirac operator in combination with accidental "bumps" in the associated wave functions at the positions of the operators.

6. Conclusions

The numerical simulations reported in this paper lend further support to the proposition that the low-lying eigenvalues of the Dirac operator in the β -regime of QCD are distributed according to the chiral unitary random matrix model. Detailed agreement has been observed, in different topological sectors, on all lattices with linear extent L larger than about 1.5 fm.

Random matrix behaviour sets in rather rapidly when going from small to large volumes. To some extent this can be understood by noting that the average of the lowest eigenvalue in the vacuum sector is inversely proportional to the volume. On the lattices A_1 , B_1 and C_1 , for example, the renormalized spectral gap

$$= Z_S^{-1} h_{1i_0} \quad (6.1)$$

in the \overline{MS} scheme at $\beta = 2$ GeV is approximately equal to 91, 23 and 8 MeV respectively. Clearly the β -regime has been safely reached on C_1 , while this is not so in the case of the lattice A_1 .

Our results also suggest that the lattice theory scales coherently to the continuum limit in all topological sectors (as is usually assumed). More extensive simulations would, however, be needed, to be able to take the continuum limit of the topological susceptibility and other quantities with confidence. This is technically possible but requires significant computer resources, since the numerical effort in these calculations tends to grow roughly proportionally to $(L/a)^4$ ($L=r_0$)⁴.

We are indebted to Poul Damgaard, Pilar Hernandez, Karl Jansen, Laurent Lelouch, Ferenc Niedermayer and Giancarlo Rossi for helpful discussions. The simulations were performed on PC clusters at DESY (Hamburg, the Institut für Theoretische Physik at the University of Bonn, the Max-Planck-Institut für Physik in München, the Max-Planck-Institut für Plasmaphysik in Garching, and the Leibniz-Rechenzentrum der Bayerischen Akademie der Wissenschaften). We wish to thank all these institutions for supporting our project and the staff of their computer centres (particularly Peter Breitenlohner, Isabel Campos and Andreas Gellrich) for technical help. L.G. was supported in part by the EU under contract HPRN-CT-2000-00145 Hadrons/LatticeQCD.

References

- [1] J. Gasser, H. Leutwyler, Phys. Lett. B 188 (1987) 477; Nucl. Phys. B 307 (1988) 763
- [2] H. Leutwyler, A. Smilga, Phys. Rev. D 46 (1992) 5607
- [3] E. V. Shuryak, J. J. Verbaarschot, Nucl. Phys. A 560 (1993) 306
- [4] J. J. Verbaarschot, I. Zahed, Phys. Rev. Lett. 70 (1993) 3852
- [5] J. J. Verbaarschot, Phys. Rev. Lett. 72 (1994) 2531
- [6] J. J. Verbaarschot, T. Wettig, Annu. Rev. Nucl. Part. Sci. 50 (2000) 343
- [7] P. H. Damgaard, Nucl. Phys. B (Proc. Suppl.) 106 (2002) 29
- [8] S. M. Nishigaki, P. H. Damgaard, T. Wettig, Phys. Rev. D 58 (1998) 087704
- [9] P. H. Damgaard, S. M. Nishigaki, Phys. Rev. D 63 (2001) 045012 [for an important correction see hep-th/0006111]
- [10] L. Giusi, C. Hoelbling, M. Luscher, H. Wittig, Comput. Phys. Commun. 153 (2003) 31
- [11] L. Giusi, P. Hernandez, M. Laine, P. Weisz, H. Wittig, in preparation
- [12] P. H. Ginsparg, K. G. Wilson, Phys. Rev. D 25 (1982) 2649
- [13] D. B. Kaplan, Phys. Lett. B 288 (1992) 342; Nucl. Phys. B (Proc. Suppl.) 30 (1993) 597

- [14] Y . Sham ir, Nucl. Phys. B 406 (1993) 90
- [15] V . Furm an, Y . Sham ir, Nucl. Phys. B 439 (1995) 54
- [16] P . Hasenfratz, Nucl. Phys. B (Proc. Suppl.) 63 (1998) 53; Nucl. Phys. B 525 (1998) 401
- [17] P . Hasenfratz, V . Laliena, F . Niedermayer, Phys. Lett. B 427 (1998) 125
- [18] H . Neuberger, Phys. Lett. B 417 (1998) 141; *ibid.* B 427 (1998) 353
- [19] M . Luscher, Phys. Lett. B 428 (1998) 342
- [20] P . Hernandez, K . Jansen, M . Luscher, Nucl. Phys. B 552 (1999) 363
- [21] R . G . Edwards, U . M . Heller, J . E . Kiskis, R . Narayanan, Phys. Rev. Lett. 82 (1999) 4188; Phys. Rev. D 61 (2000) 074504
- [22] P . H . Damgaard, R . G . Edwards, U . M . Heller, R . Narayanan, Phys. Rev. D 61 (2000) 094503
- [23] P . Hasenfratz, S . Hauswirth, T . Jorg, F . Niedermayer, K . Holland, Nucl. Phys. B 643 (2002) 280
- [24] W . Bietenholz, K . Jansen, S . Shcheredin, JHEP 0307 (2003) 033
- [25] B . Bunk, K . Jansen, M . Luscher, H . Simma, Conjugate gradient algorithm to compute the low-lying eigenvalues of the Dirac operator in lattice QCD, notes (September 1994)
- [26] T . Kalkreuter, H . Simma, Comput. Phys. Commun. 93 (1996) 33
- [27] R . Sommer, Nucl. Phys. B 411 (1994) 839
- [28] S . Necco, R . Sommer (ALPHA collab.), Nucl. Phys. B 622 (2002) 328
- [29] L . DelDebbio, C . Pica, hep-lat/0309145
- [30] C . Alexandrou, E . Follana, H . Panagopoulos, E . Vicari, Nucl. Phys. B 580 (2000) 394
- [31] S . Capitani, L . Giusi, Phys. Rev. D 62 (2000) 114506
- [32] P . Hernandez, K . Jansen, L . Lellouch, H . Wittig, JHEP 0107 (2001) 018; Nucl. Phys. B (Proc. Suppl.) 106 (2002) 766